



The impact of biochar amendment on soil water infiltration and evaporation under climate change scenarios

Arwan Apriyono¹ · Yuliana Yuliana² · Zhongkui Chen³ · Suraparb Keawsawasvong⁴ · Viroon Kamchoom²

Received: 9 August 2023 / Accepted: 2 January 2024 / Published online: 25 February 2024

© The Author(s) under exclusive license to Institute of Geophysics, Polish Academy of Sciences & Polish Academy of Sciences 2024

Abstract

Biochar is an eco-friendly material that is potentially used in earthworks to prevent stability and serviceability problems under extreme scenarios. This study aims to examine the effects of biochar amended on water infiltration and evaporation under extreme climate. A series of numerical analyzes were conducted to observe the response of pore water pressure (PWP) to extreme climate variation with an application of biochar composition. Moreover, an analysis of variance (ANOVA) has been performed to investigate the effect of biochar on soil water holding capacity at a low suction range. According to the result, biochar amended can maintain the fluctuation of PWP due to wetting and drying processes under extreme climate scenarios. This is due to the fact that the finer particles of biochar may clog large soil pores, reducing the water infiltration rate. Moreover, the addition of biochar can increase water retention capacity at low matric suction ranges, which can prevent flooding during extreme wet conditions. Further to this, the addition of biochar to the soil can maintain PWP fluctuation at the near surface area under extreme climate, preventing soil desiccation cracks.

Keywords Biochar soil enhancement · Earthworks · Extreme climate · Soil hydrology · Numerical simulation

Introduction

Water infiltration and evaporation are the main factors that should be taken into account in embankment stability and serviceability analysis. It is widely known that water infiltration can cause stability issues in numerous earthworks, including embankments and cut fills (Fredlund and Rahardjo 1993; Ranjan and Rao 2000; Briggs et al. 2019).

The infiltration may reduce soil strength as a result of the increase in pore water pressure (PWP), leading to slope instability (Briggs et al. 2013; Lees et al. 2013; Apriyono et al. 2023). Moreover, the cycle of water infiltration and evaporation during seasonal variation can lead to the fluctuation of PWP (Chen et al. 2022a, 2023a; Dong et al. 2023). The larger range of PWP fluctuation has a significant impact on slope serviceability, triggering progressive failure (Leroueil 2001; Smethurst et al. 2006; Glendinning et al. 2014). Further to this, extreme climate as a result of climate change is undeniable and will exacerbate stability and serviceability issues. Recently, Zeng et al. (2020) and Cheng et al. (2021) stated that prolonged drought can increase the water infiltration rate due to the attendance of the cracks. Likewise, evaporation can also rise during extreme drought conditions through the occurrence of desiccation cracks (Cui et al. 2014; Song and Cui 2020). Given the aforementioned issues, it is of utmost importance to explore environmentally-friendly solutions for controlling water infiltration and evaporation to effectively prevent earthworks stability problems.

Biochar, a substance derived from biomass (such as peanut shells, wheat straw, and wood chips) through heating in a low-oxygen environment, is commonly used to address soil and environmental issues due to its unique properties

Edited by Dr. Hossein Hamidifar (ASSOCIATE EDITOR) / Prof. Jochen Aberle (CO-EDITOR-IN-CHIEF).

✉ Viroon Kamchoom
viroon.ka@kmitl.ac.th

¹ Civil Engineering Department, Jenderal Soedirman University, Purwokerto, Indonesia

² Excellent Center for Green and Sustainable Infrastructure, School of Engineering, King Mongkut's Institute of Technology Ladkrabang, Bangkok 10520, Thailand

³ Shenzhen Yanzhi Science and Technology Co., Ltd, Shenzhen 518101, China

⁴ Research Unit in Sciences and Innovative Technologies for Civil Engineering Infrastructures, Department of Civil Engineering, Thammasat School of Engineering, Thammasat University, Pathumthani 12120, Thailand

and numerous beneficial effects on soil and surrounding ecosystems (Lehmann and Joseph 2009). In the field of agriculture, biochar can lead stimulation of growth, activity, and metabolic efficiency of the microbial biomass, including plant symbionts (George et al. 2012). Moreover, due to its ability to absorb and reduce methane emissions through microbial methane oxidation and immobilize certain pollutants and heavy metals in the soil, biochar can be employed as a final cover in landfills (Shang et al. 2013; Yu et al. 2013; Wong et al. 2017). In terms of physical properties, incorporating biochar into soil mixtures can enhance water retention capacity and hydraulic conductivity owing to its porosity (Wong et al. 2017; Chen et al. 2020, 2023b; Garg et al. 2021). Moreover, regarding Razzaghi et al. (2020) and Wang et al. (2022), biochar amended soil mixtures can significantly reduce water infiltration capacity. It can be attributed to the high surface area and pores of biochar, permitting it to be first filled up before the gravitational moisture percolates down. Furthermore, the finer particles of biochar can clog the large soil pores, resulting in pore blockage and thus reducing water infiltration rate. Further to this, the use of biochar as a soil improvement led to a decrease in evaporation (Feng et al. 2023). This reduction can be attributed to biochar's porous structure, which enhances the capacity for capillary water retention in soil voids, thereby improving the soil's resistance to evaporation.

To date, the majority of research has focused on the effect of biochar addition on crop soil water infiltration in arid and semiarid locations (Abrol et al. 2016; Novak et al. 2016; Ibrahim et al. 2017). In their research, loosely compacted soil was used in association with the requirement of soil respiration for plant growth (Passioura 2002; Kamchoom et al. 2022). In the context of earthwork, several researchers studied the effect of biochar on embankment. Due to its lightweight and moisture-retentive properties, biochar-amended soil has the potential to enhance earthwork stability, particularly in embankments (Lagmago 2021; Hussain and Ravi 2022; Ramezanzadeh et al. 2023). Hussain and Ravi (2022) stated that biochar-amendment soil decreased the dry unit weight. Moreover, the biochar-amended soil improved plant roots, thus increasing slope stability (Ng et al. 2017; Kamchoom and Leung 2018). Recently, Chen et al. (2022b) proposed that biochar-amended soil could potentially serve as landfill cover in waste disposal systems. Based on their research, the application of biochar can reduce the thickness of soil cover, leading to a decrease in water infiltration and percolation. Regarding Ramezanzadeh et al. (2023), the application of biochar amended soil has a great contribution in enhancing the definite range of aggregation formation. However, the addition of biochar can reduce soil compaction, hence decreasing shear strength. Based on Lagmago (2021), sand-biochar mixtures are potentially used as fill material for roadways with respect to satisfactory drainage

properties. Since the increment in biochar composition is not promising to enhance the physical properties of soils, it is necessary to find a balance between the consumption of biochar and its effect on soil–water retention. To date, there is limited research on the application of biochar to prevent serviceability problems in earthworks, particularly under extreme climate variations. Given that the embankment will undergo wetting and drying cycles, additional studies are needed to investigate the behavior of biochar-amended soils in response to seasonal variations.

The objective of this study is to investigate the water infiltration and evaporation of biochar-amended soil (BAS) under extreme climate scenario variation. In order to conduct this investigation, three variations of biochar composition (0, 10, and 20%) were observed. Moreover, excessive rainfall and drought based on the worst Thailand climate scenario (RCP 8.5) in the near future (2030) and far future (2060) were implemented in this simulation. The current climate condition was also applied in the simulation for comparison purposes. A finite element model was used to investigate transient seepage analysis. Water infiltration rate and evaporation have been subjected in the model in relation to biochar composition and climate scenarios. Moreover, PWP along the depth was also investigated in this study with respect to biochar composition and climate variation. This research is expected to provide a better knowledge of the use of BAS to prevent stability and serviceability problems of earthwork, particularly under extreme climate scenarios.

Methodology

Model geometry

To obtain the research aim, a numerical study was simulated considering an experimental model which was conducted by Chen et al. (2022a). In their research, a soil column with a diameter of 0.28 m, and a height of 0.7 m was generated to study water infiltration in BAS. Accordingly, axisymmetric idealization was used in this simulation, measuring the radius of 0.14 m and the height of 0.7 m as illustrated in Fig. 1. The height of the model was determined from the commonly-used thickness of landfill cover, ranging between 0.45 and 1.2 m (Albright et al. 2006). Moreover, to facilitate the investigation, four observation points were determined in the model, located at the depths of 0.05, 0.25, 0.45, and 0.65 m, representing near surface area, two points of middle area and the deepest depth. Following this, since one dimensional axisymmetric idealization was used in this analysis, the width of the model has been set as minimum as possible hindering lateral behavior distraction. Furthermore, this study simulated three variations of BAS composition, namely B0, B10, and B20, representing biochar composition

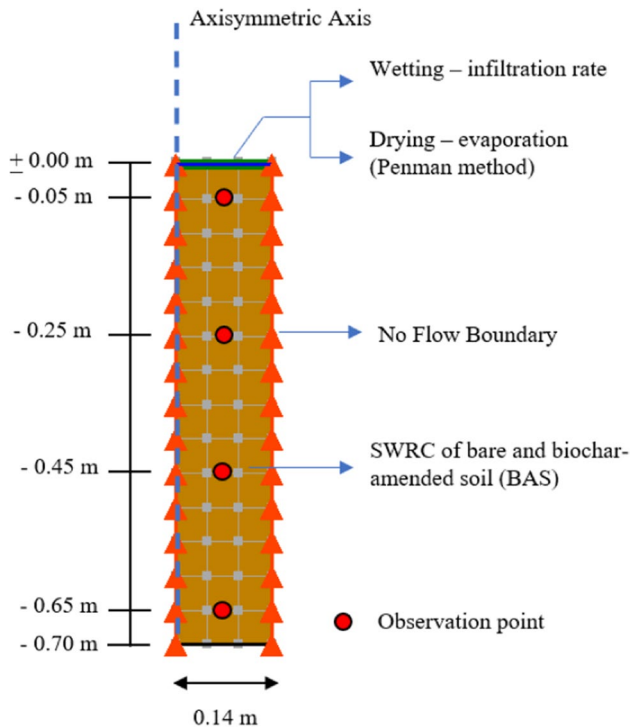


Fig. 1 Model Geometry

of 0, 10, and 20%. Regarding Jin et al. (2016), the addition of 10 or 20% biochar suggests the possibility of interaction between biochar and soil components and/or the influence of biochar oxidation.

Material properties

The biochar utilized in this investigation was purchased in China from Shangqiu Sanli New Energy Co., Ltd. It was generated by slow pyrolysis from agricultural waste (specifically, peanut shell) with a heating rate of 5–10 °C min⁻¹ maintained at that temperature for 30–40 min, or until 500 °C was reached. In order to extract biochar with a particle size smaller than 0.25 mm, it was ground to pass through a 0.25 mm sieve. To eliminate any residual moisture and ensure precise mass fractions, all test materials (silty sand and peanut shell biochar) were dried in an oven at 105 °C for a duration of 24 h. The soil utilized in the simulation was fully decomposed granite (CDG), which was commonly used as building material in Thailand, China, and other countries. Soil properties in this study were obtained from laboratory tests, performed by Chen et al. (2022a). The soil was classified as silty-sand (SM) consisting of sand (57.4%), silt (27.6%), and clay (15%), based on The Unified Soil Classification System (USCS). In addition, the biochar used in this study was ground to pass through a 0.25 mm sieve, resulting in biochar with a particle size smaller than 0.25 mm.

Considering ASTM D854-14 (2003), biochar composition of 0, 10, and 20% resulted from specific gravity of 2.62, 2.56, and 2.51, respectively. Due to the lower dry density of biochar particles compared to soil particles, an increase in biochar application resulted in a decrease in specific gravity. Specifically, biochar applications of 0, 10, and 20% led to maximum dry densities of 1.66, 1.48, and 1.43 g/cm³, respectively. However, the corresponding optimum water content was increased as more pores from biochar were presented in the BAS. Regarding the mercury intrusion porosimeter test result, compared to biochar 0%, the total pore volume was increased by about 15 and 40% as the biochar application of 10 and 20% respectively. Moreover, the application of biochar transformed the saturated hydraulic conductivity (K_{sat}) of soil. Regarding Chen et al. (2022a), the addition of biochar of 10% and 20% decreased the value of K_s by about 41.9% (7.17⁻⁷ m/s) and 48.9% (5.67⁻⁷ m/s) respectively, compared to bare soil (1.24⁻⁶ m/s).

To conduct transient seepage analysis, the soil water retention curve (SWRC) and hydraulic conductivity function (HCF) were required. Accordingly, the correlation between soil suction and volumetric water content (VWC) was used to generate SWRC. In this research, both drying and wetting SWRC were deployed which were obtained from laboratory experiments, conducted by Chen et al. (2022a). Measured SWRC data were fitted using the Genuchten model (Van Genuchten 1980), following Eq. (1). Equation (2) was then used to predict HCF based on SWRC and saturated hydraulic conductivity. Measured and fitted SWRC during the wetting and drying process based on experimental data can be depicted in Fig. 2.

$$\theta = \theta_r + \frac{(\theta_s - \theta_r)}{((1 + a\psi)^n)^m}, \quad (1)$$

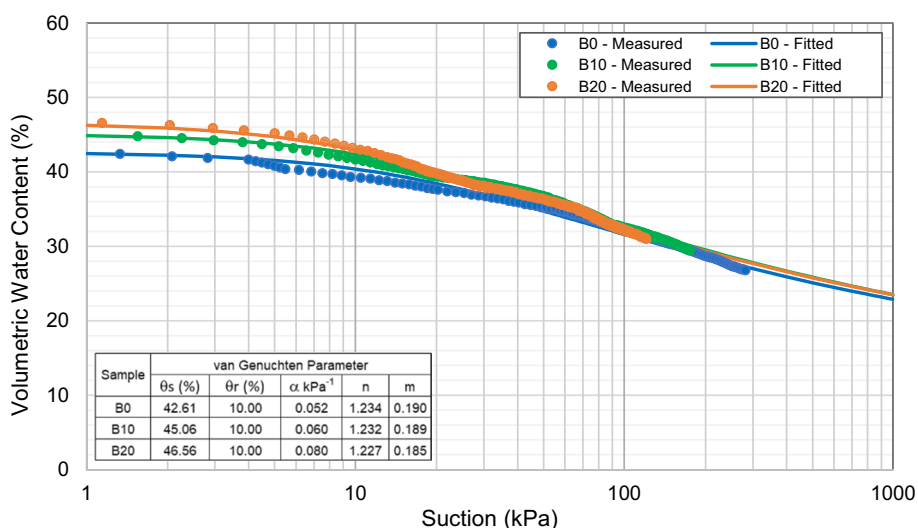
where θ is VWC (%), θ_s is saturated VWC (%), θ_r is residual VWC (%), ψ is matrix suction and a , n , m is curve fitting parameters.

$$K_w = K_{sat} \frac{[1 - (a\psi^{(n-1)})(1 + (a\psi^n)^{-m})]^2}{((1 + a\psi^n)^n)^{\frac{m}{2}}}, \quad (2)$$

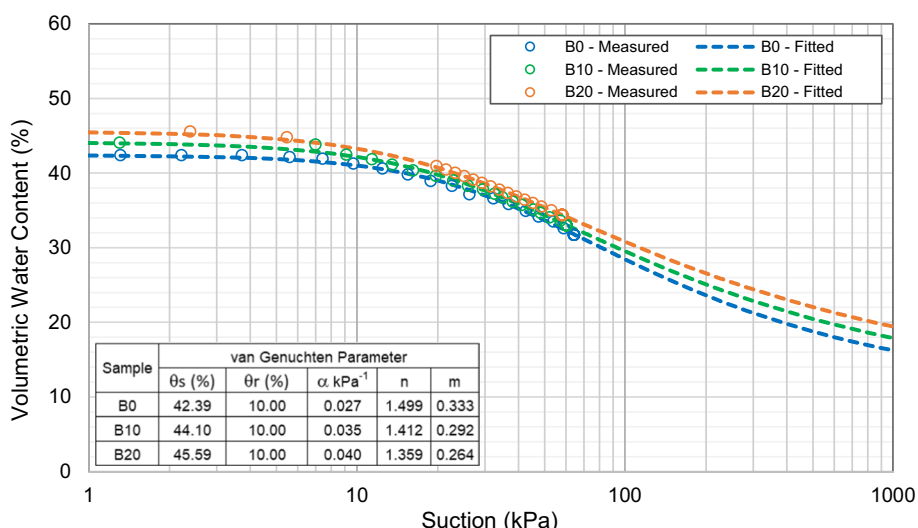
where K_w is unsaturated hydraulic conductivity (m/sec).

It can be seen in Fig. 2 that SWRC varied in accordance with BAS composition. Moreover, the wetting and drying process resulted in a subtle SWRC pattern, represented in Fig. 2a and b respectively. Figure 2 shows that wetting SWRC tend to have lower saturated and residual VWC, as well as steeper slope gradient, compared to drying part. With biochar application rates of 10 and 20%, the saturated water content increased by approximately 2.5 and 4%, respectively. The increase in water content was proportional to the rise in porosity. With a larger pore volume and greater surface area,

Fig. 2 SWRC (a) Drying (b) Wetting



(a)



(b)

a higher biochar application rate enhances its water absorption capabilities during infiltration, thereby increasing its water-holding capacity (Uzoma et al. 2011). On the other hand, the impact of biochar composition on the air-entry values and absorption curves was found to be limited. This suggests that the size and distribution of pores in the biochar-amended soil (BAS) remained largely unchanged compared to the bare soil sample. As a result, the alterations in air-entry values and absorption curves were negligible. The experimental measurements were fitted with the van Genuchten model and subsequently utilized in the numerical modeling.

Boundary condition

No flow boundary was set on the right and left sides of the model, representing an impermeable wall of the column.

Moreover, the review boundary was situated at the bottom of the model (i.e., seepage boundary during rainfall and no flow boundary during evaporation). Further to this, the model was subjected to rainfall and evaporation to represent the wet and dry seasons. The Green-Ampt (GA) infiltration method was used (Green and Ampt 1911) to calculate the water flux boundary with regard to precipitation. According to Cui and Zhu (2017) the GA model is more commonly used in many applications as it considers more physical parameters such as saturated hydraulic conductivity (K_{sat}), PWP, and VWC, thus resulting in better accuracy, compared to other models. However, the measurement of K_{sat} should be performed prior to the calculation. The infiltration rate and cumulative infiltration depth can be calculated using Eqs. (3) and (4). It should be noted that the GA parameter was obtained from a laboratory experiment, conducted by Chen et al. (2022a).

In addition, the Penman method (Penman 1948) was used to calculate evaporation based on Thailand climate data as can be depicted in Eq. (5). Based on Allen et al. (1998), since Penman method uses standard climatological records of solar radiation (daylight), air temperature, humidity and wind speed this method is more relatively convenient to determine evaporation value, rather than field measurement experiment. However, this model is less accurate than that direct evaporation test such as pan evaporation.

$$F(t) = K_{sat}t + \psi \Delta \theta \ln \left(1 + \frac{F(t)}{\psi \Delta \theta} \right), \quad (3)$$

$$f(t) = K_{sat} \left(\frac{\psi \Delta \theta}{F(t)} + 1 \right), \quad (4)$$

where $f(t)$ is infiltration rate (mm/sec), t is time (sec), ψ is suction head (mm), and $\Delta \theta$ deficit of VWC.

$$PET = \frac{0.408 \Delta \cdot (Rn - G) + \gamma \frac{900}{T+273} u_2 (e_s - e_a)}{\Delta + \gamma (1 + 0.34 u_2)}, \quad (5)$$

where PET is Potential Evaporation (mm/day), Rn is Net Radiation (MJ/m²day), G is Soil heat flux density (MJ/m²day), T is Mean daily air temperature at 2 m height (°C), u_2 is Wind speed at 2 m height (m/sec), e_s is saturation vapor pressure (kPa), e_a is actual vapor pressure (kPa), Δ is slope vapor pressure curve (kPa/°C), γ is psychrometric constant (0.061 kPa/°C).

In terms of the extreme climate scenario, the future projection of the twenty-first century was calculated based on the 1956–2000 data series (Qiao et al. 2021). Moreover, considering the alteration of surface air temperature, two future periods were defined, representing future climate, i.e., near future from 2026 to 2045, and far future from 2041 to 2060. Based on their study, air temperatures will increase by approximately 1.64 and 2.09 °C in the near and far future, respectively. Accordingly, three variations of extreme climate scenarios were implemented in this study i.e., current climate, near future (2030), and far future (2060), regarding the worst case scenario in Thailand. Since having distinct climate conditions, the study of the biochar effect on water infiltration and evaporation based on those three climate scenarios will provide a profound contribution to this field of study. Further to this, rainfall intensity and duration used in this research were derived from Thailand intensity duration frequency (IDF), developed by Yamoat et al. (2022) as can be seen in Fig. 3. Pertaining to their research, Thailand will be experienced with maximum hourly rainfall intensity of 19.2 mm/h for 12 h regarding 100 years return period. Considering the same rainfall intensity, 4 and 8-h duration of rainfall represented 2 and 10 years return periods respectively. Note that Intensity Duration Frequency (IDF) has been

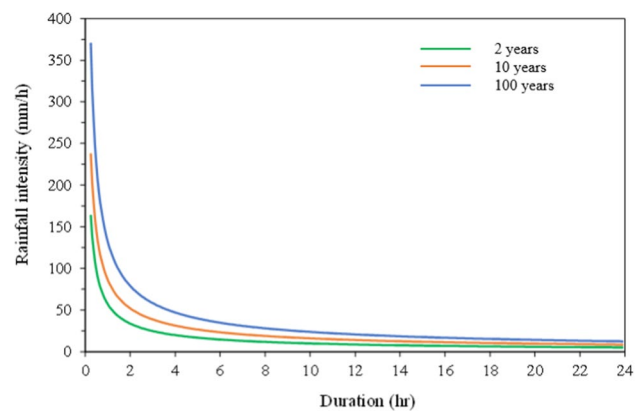


Fig. 3 Thailand intensity duration frequency (After Yamoat et al. (2022))

derived based on 30 years (1990–2020) historical data. Further to this, based on Shrestha et al. (2017) maximum rainfall intensity will increase by about 37.9 and 54.9% in the near future (2030) and far future (2060). Therefore, the model will be subjected to 27.5 and 31.0 mm/h during extreme near and far future scenarios respectively.

In the context of evaporation, weather data was required in the calculation with regard to three extreme climate scenarios. World Bank Group and The Asian Development Bank (2021) reported that the atmospheric condition will remarkably change with time, considering the worst climate scenario (RCP 8.5). Based on their analysis, the average of air temperature was about 32.3, 34.8, and 37.5 °C during current, near and far future scenarios. Moreover, the mean of air humidity will gradually decrease by approximately 81.39, 80.39, and 78.39% during current, near and far future conditions respectively. In accordance with those atmospheric data, it can be reported that the model was subjected to evaporation of 5.08, 5.42, and 5.81 during current, near and far future climate scenarios. Those evaporations were implemented into the model to simulate drying conditions. All of input parameters to calculate water infiltration and evaporation can be seen in Table 1.

Analysis procedure

A series of numerical analyzes were done to compare the PWP response during rainfall and evaporation events using Seep/W. Seep/W is a highly effective finite element modeling software for predicting groundwater flow in a porous medium. SEEP/W is capable of simulating both basic saturated steady-state problems and complex saturated/unsaturated transient analyzes with atmospheric interaction at the ground surface. Each simulation consists of three stages: (i) steady state analysis to determine the initial PWP for each model; (ii) transient seepage analysis owing to rainfall; and

Table 1 Water infiltration and evaporation parameter

Sample	Green Ampt Infiltration Parameter						Penman Parameter				
	Current Climate						Current Climate				
	θ_e	K_s (mm/hr)	Se	$\Delta\theta$ (%)	i (mm/hr)	T (°C)	Rh (%)	Rs (MJ/m ² day)	γ (kPa/°C)	Δ	
B0	0.43	4.46	0.430	1.162	19.20	32.36	81.39	24.08	0.061	0.230	
B10	0.44	2.58	0.450	1.169	19.20	32.36	81.39	24.08	0.061	0.230	
B20	0.47	2.04	0.460	1.167	19.20	32.36	81.39	24.08	0.061	0.230	
	Near Future Climate						Near Future Climate				
B0	0.43	4.46	0.430	1.162	27.50	34.86	80.39	24.27	0.061	0.230	
B10	0.44	2.58	0.450	1.169	27.50	34.86	80.39	24.27	0.061	0.230	
B20	0.47	2.04	0.460	1.167	27.50	34.86	80.39	24.27	0.061	0.230	
	Far Future Climate						Far Future Climate				
B0	0.43	4.46	0.430	1.162	31.00	37.56	78.39	24.32	0.061	0.230	
B10	0.44	2.58	0.450	1.169	31.00	37.56	78.39	24.32	0.061	0.230	
B20	0.47	2.04	0.460	1.167	31.00	37.56	78.39	24.32	0.061	0.230	

(iii) transient seepage analysis due to evaporation throughout the drying phase. Initial PWP was determined in steady-state phases based on the PWP value at the commencement of the test. To analyze wet conditions, the model was subjected to precipitation for 12 h. The values of PWP were observed at the time of 4, 8, and 12 h, representing a return period of 2-years, 10-years, and 100-years respectively. Following this, evaporation based on Penman calculation was applied in the drying simulation for 144 h. Further to this, extreme rainfall and evaporation induced by current, near future, and far future extreme climate were also applied to the model. Following numerical simulation, Analysis of Variance (ANOVA) has been deployed to investigate water holding capacity based on SWRC curves. Regarding Sawyer (2009), ANOVA is a statistical tool used to detect differences between experimental group means. ANOVA is based mathematically on linear regression and general linear models that quantify the relationship between the dependent variable and the independent variable. In this analysis, negative PWP (suction) was divided into three range groups, i.e., < 10 kPa, 10–50 kPa and 51–100 kPa, representing very low, low and medium level suction (Pham et al. 2023).

Result and discussion

Effects of biochar on infiltration rate

The value of infiltration rate and cumulative infiltration depth over time, based on the GA method can be plotted in Fig. 4. The infiltration rate represents the velocity at which water enters the soil. Meanwhile, cumulative infiltration depth equals the water amount that infiltrated to the soil at a specific time. Figure 4a, b and c correspond to the

calculation result of biochar content 0, 10, and 20%, respectively. Furthermore, the graph also showcases three distinct climate scenarios: current, near future, and far future. Regarding Fig. 4, it becomes apparent that at the beginning of rainfall, the water infiltration rate is relatively high due to the substantial difference in hydraulic gradient between the upper and lower soil layers. Subsequently, the infiltration rate decreases significantly as the hydraulic gradient decreases, eventually reaching a stable condition. Overall, it can be inferred that the application of biochar reduces the water infiltration rate, consequently diminishing the infiltration depth. This phenomenon can be attributed to the higher porosity of the biochar-amended soil (BAS) column, which enables greater water absorption compared to bare soil. In the context of the current climate scenario, the application of 10% and 20% biochar results in a reduction of water infiltration rate by approximately 33.9% (4.35×10^{-7} m/s) and 42.2% (3.81×10^{-7} m/s) respectively, compared to bare soil (6.58×10^{-7} m/s). As such, reducing water infiltration depth by about 31.1% (11.2 mm) and 38.5% (13.9 mm) respectively. This is due to the fact that finer particles of biochar may clog large soil pore, reducing water infiltration rate (Ibrahim et al. 2017). Moreover, regarding Ibrahim et al. (2013) biochar can be considered as a binding agent, leading to flocculate soil particles to form stable aggregates and thus limiting the downward movement of soil water.

Besides, Fig. 4 also shows the infiltration rate of near and far future extreme climate scenarios. It can be seen in Fig. 4 that infiltration rates under future extreme climates tend to have a similar pattern to the current climate. However, future extreme climate resulted from a higher infiltration rate significantly compared to the current climate for all of three BAS variations in association with the increase in rainfall intensity. Without biochar application, the near and far future

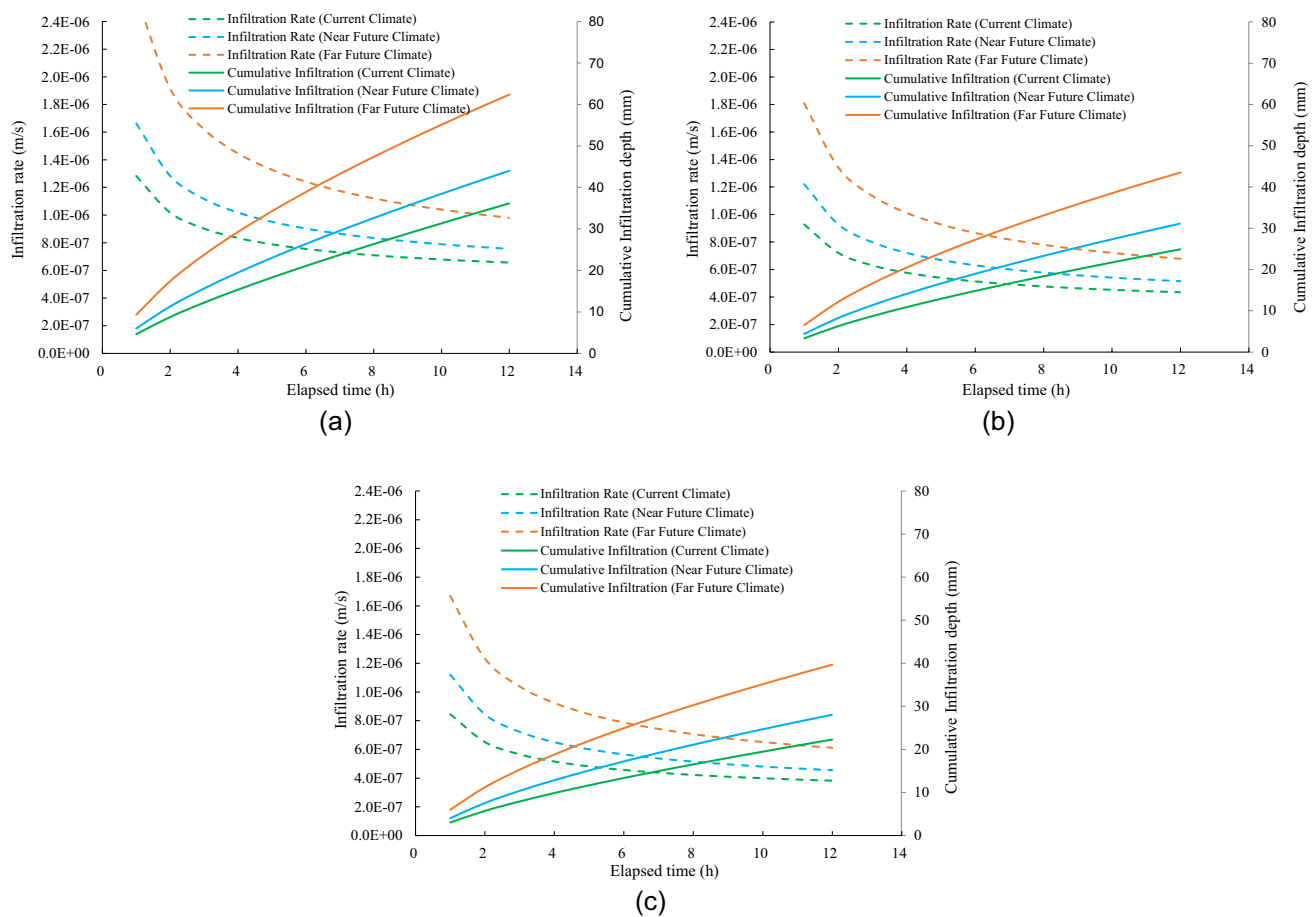


Fig. 4 Infiltration rate and cumulative infiltration (a) B0 (b) B10 (c) B20

extreme climate will trigger the increase in infiltration rate by about 15% (7.57×10^{-7} m/s) and 49% (9.83×10^{-7} m/s), compared to the current climate scenario (6.58×10^{-7} m/s). On the other hand, the application of biochar 10% and 20% can reduce infiltration rate under near future extreme climate scenarios by approximately 32% (5.14×10^{-7} m/s) and 40% (4.56×10^{-7} m/s) as compared with bare soil (7.57×10^{-7} m/s). Likewise, the increasing of biochar composition to 10% and 20% can lead to the reduction of water infiltration rate by around 31% (6.77×10^{-7} m/s) and 38% (6.10×10^{-7} m/s), compared to bare soil column (9.83×10^{-7} m/s) during the far future extreme climate. Given the result that the biochar amendment can reduce water infiltration, it has the possibility of providing a more effective design of landfill cover. It is due to the fact that the application of biochar as a soil mixture can reduce landfill cover thickness, and hence minimizing the budget.

The response of PWP due to extreme wet climate with biochar variation

Figure 5 illustrates the response of PWP along the depth during rainfall with the application of three biochar compositions under three extreme climate scenarios. The fluctuation of PWP due to the application of biochar 0, 10, and 20% can be depicted in Fig. 5a, b, and c respectively. At the beginning of the simulation, the initial PWP was set by about -60 kPa following experimental data. As water infiltrated into the soil, the PWP along the depth gradually increased. It can be seen in Fig. 5 that the PWP at 0.05 m depth jumped to near 0 kPa in all variations of biochar composition after 8 h of rainfall, under the current climate scenario. The value of PWP becomes less fluctuated at the deeper depth in association with water infiltration depth. The current climate scenario promoted the increase in PWP up to the depth of 0.25 m in bare soil (30%), indicating maximum water infiltration depth. Noted that the PWP value at a depth of

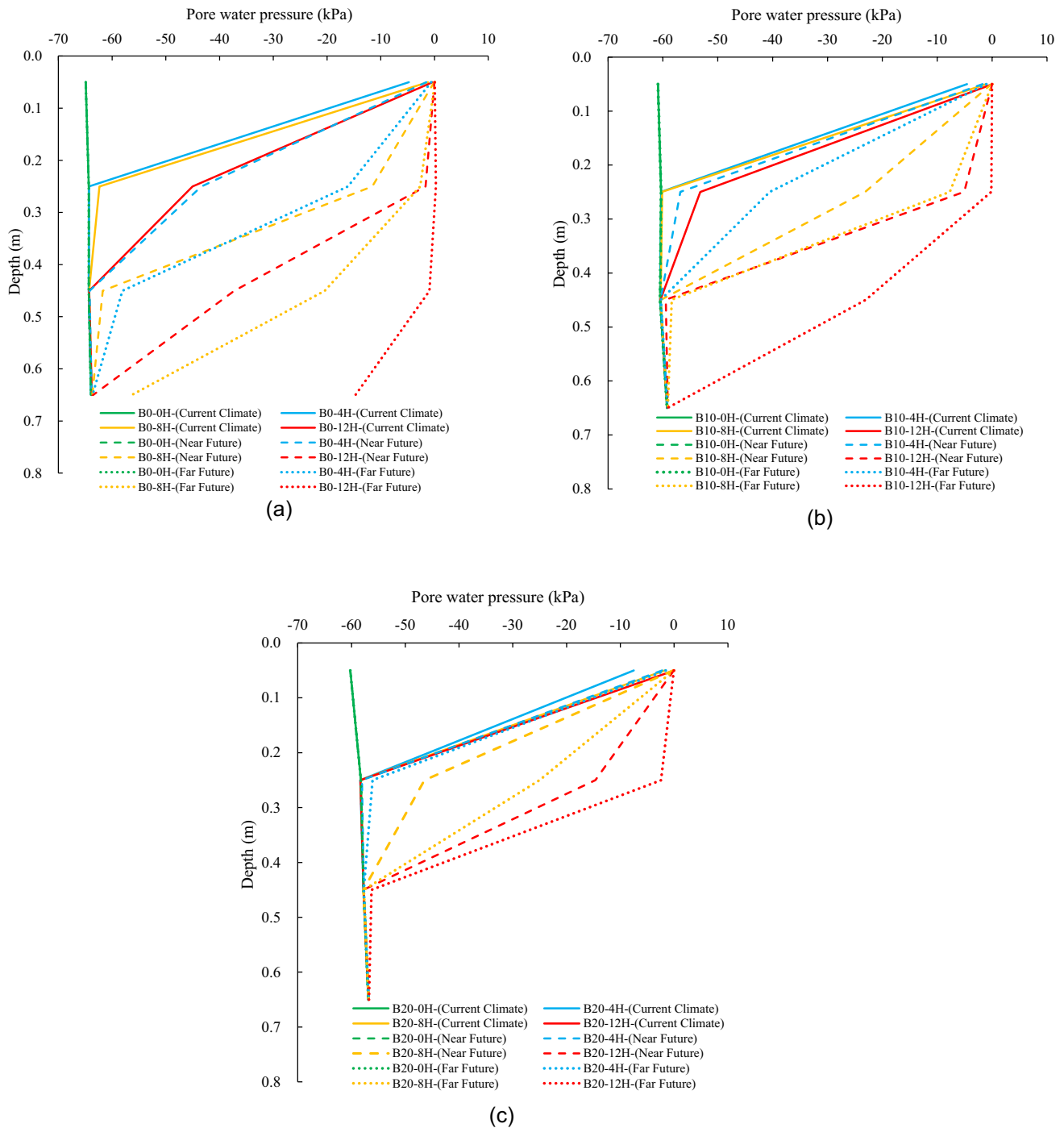


Fig. 5 Development of pore water pressure (PWP) with depth during rainfall (a) B0 (b) B10 (c) B20

0.45 m has remained unchanged due to the application of all biochar composition under the current climate scenario. On the other hand, biochar application of 10% can retain PWP value significantly to the depth of 0.25 m (11%). In fact, the value of PWP at 0.25 m depth is almost similar after 12 h of rainfall with the biochar application of 20%. It indicated that

the biochar application of 10% and 20% can reduce water infiltration depth significantly.

Future extreme climate scenarios triggered remarkable fluctuation of PWP, compared to the current climate as can be depicted in Fig. 5. Without biochar application, water infiltrated to the depth of 0.45 m after 12 h of

rainfall due to the near future extreme climate, leading to the increase in PWP by about 42% (−37.2 kPa). Moreover, the application of biochar 10% can maintain PWP to the depth of 0.45 m, minimizing the increase in PWP by approximately 2% (−59.5 kPa). Further to this, the value of PWP was unchanged at 0.45 m depth as the application of biochar 20% under near future extreme climate scenarios. It was substantiated that the addition of biochar 20% can prevent water percolation up to the depth of 0.45 m under near future extreme climate scenarios. In the context of far future extreme climate, rainfall led to an increase in PWP value up to the depth of 0.65 m after 12 h of rainfall in bare soil (77%). However, the application of biochar 10% and 20% significantly influenced PWP due to far future extreme climate scenarios. It can be indicated from the constant value of PWP at the depth of 0.65 m after 12 h of rainfall under far future extreme climate with respect to biochar application of 10 and 20%. The addition of biochar 10% and 20% can promote the increase in PWP by about 61% (−23.4 kPa) and 3% (56.2 kPa) respectively at the depth of 0.45 m under far future extreme climate. It substantiated that the application of biochar 20% can prevent water percolation up to the depth of 0.45 m under far future extreme climate scenarios. This result is useful for further consideration of soil cover thickness in BAS application. Thus, the use of biochar can improve the performance of soil covers by decreasing water infiltration and enhancing water retention. Further to this, as biochar ages, it is incorporated into soil aggregates, protecting the biochar carbon and promoting stabilization (Joseph et al. 2021). Moreover, biochar is regarded as a chemically and biologically very stable carbon pool and can persist in nature for long periods of time (Cheng et al. 2008). Given that characteristic, it is evidence that biochar can reduce water infiltration of soil in long-term conditions. Based on the result, it can be suggested that the application of a 10% biochar composition can be effectively used in landfill covers, measuring 0.45 m in thickness under near future climate. Moreover, the same thickness of landfill cover can be resilient in far future climates with the implementation of 20% biochar. It should be noted that without biochar application, the thickness of landfill cover tends to be higher to prevent serviceability problems, promoting an increase in financial support.

The response of PWP due to extreme dry climate with biochar variation

The responses of PWP during the drying process with the variation of biochar composition variation under three climate scenarios can be illustrated in Fig. 6. It can be seen in Fig. 6 that the PWP value was more fluctuated at near surface depth, compared to the deeper depth due to the evaporation process. With respect to the current climate scenario, soil in the upper

half of the column was saturated, based on the previous simulation. Following this, PWP decreased after 48 h of evaporation. However, PWP in the lower layer of the column was still increased due to the downward infiltration through the column. The downward infiltration process stopped after 48 h of evaporation. Moreover, the application of biochar can maintain the decrease in PWP as compared with bare soil. Without biochar application, PWP dropped by around −188 kPa at a depth of 0.25 m under the current climate scenario. At the same depth, the application of biochar at 10 and 20% decreased the PWP value by approximately −93.5 and −45.75 kPa respectively. It can be attributed to the finer particle of biochar which decreased the soil porosity, reducing evaporation area. Regarding Feng et al. (2023) the addition of biochar 10, 30 and 50% can decrease evaporation by approximately 9.58, 10.95, and 4.2%, respectively. As PWP fluctuation during the wetting and drying process can trigger progressive failure of the embankment, maintaining PWP is required to prevent serviceability problems.

Regarding future extreme climate scenario analysis, the noticeable decrease in PWP occurred with the application of three biochar variations at near surface depth. Compared to the current climate scenario, near and future extreme climate promote the decrease in PWP value by about 23% (−232 kPa) and 95% (369 kPa) respectively at a depth of 0.25 m without biochar application. Moreover, the addition of biochar composition can also reduce the decrease in PWP significantly under extreme scenarios. Under near future extreme climate scenarios, the minimum PWP at depth of 0.25 m was around −164 kPa and −115 kPa with variations of biochar application of 10 and 20% respectively. It should be noted that the PWP value decreased by around 29 and 50%, compared to the B0 variation (−232 kPa). In terms of far future extreme climate scenarios, evaporation promoted the decreasing PWP by approximately −219 and −168 kPa due to the addition of biochar 10% and 20% at the depth of 0.25 m. Figure 6 shows the application of BAS maintained PWP value at the lower half of the column under future extreme climate scenarios as compared with B0 variation. It substantiated that biochar can mitigate PWP under extreme drought conditions. Since extreme wet and dry climates can promote the fluctuation of PWP to be more significant, promoting progressive failure in the future (Anderson and Kneale 1980; Smethurst et al. 2006) and even affecting reinforcement in soil stabilization structure (Borana et al. 2016, 2017), the application of biochar amendment is significantly important.

Responses of PWP during rainfall at BAS with return period variation

Since IDF is an important standard to represent rainfall intensity, the observation of PWP response due to return period

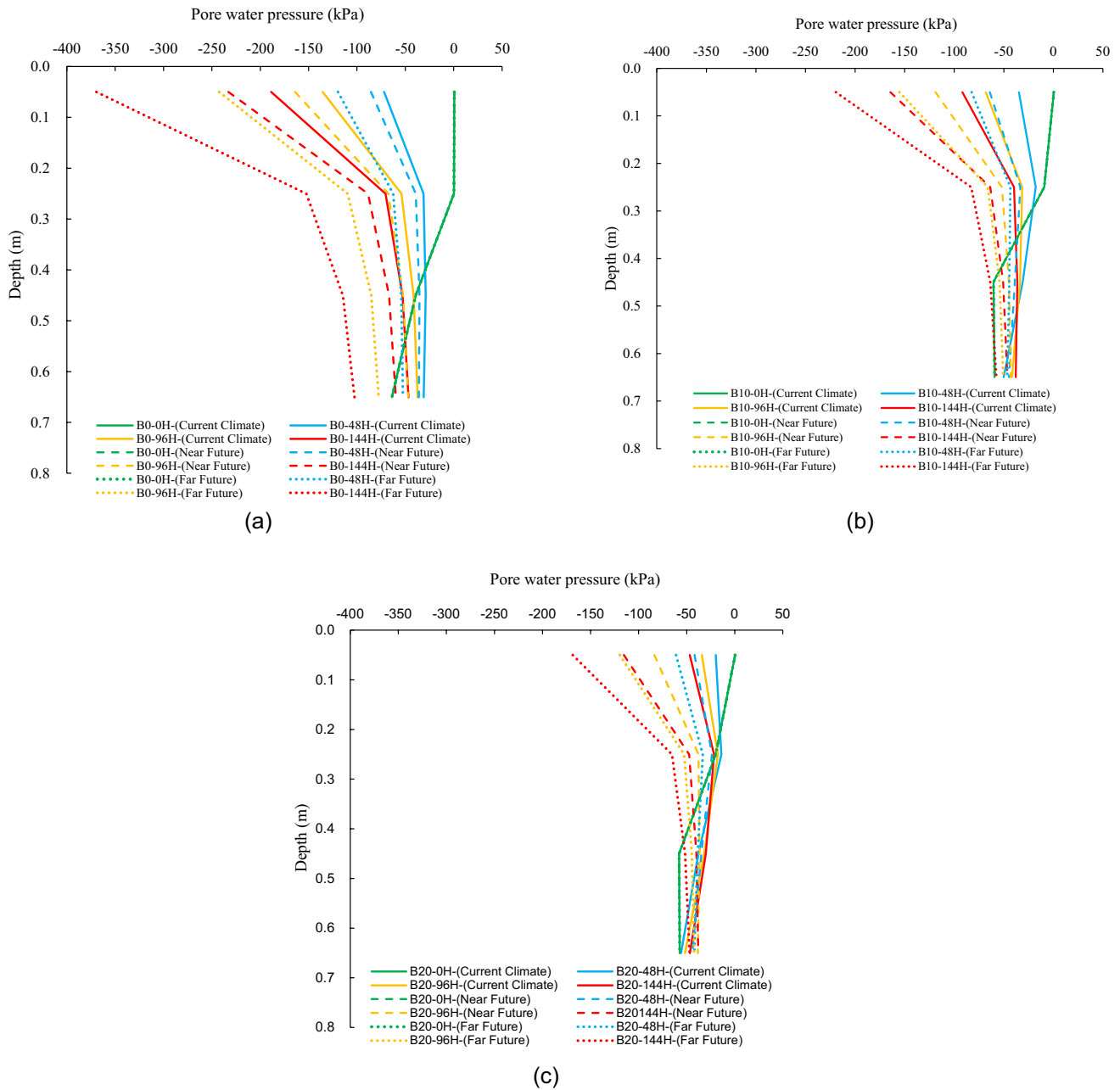


Fig. 6 Development of pore water pressure (PWP) with depth during drying **(a)** B0 **(b)** B10 **(c)** B20

variation is required. Figure 7 shows the behavior of PWP with return period variation because of biochar composition. In detail, the effect of the return period to PWP at the depth of 0.25 m due to current climate conditions can be depicted in Fig. 7a. In the context of current climate conditions, 10 years return period of rainfall can slightly infiltrate to the soil without biochar composition (B0) to the depth of 0.25 m. It can be attributed to the increase in PWP by about 3%. Moreover, PWP increased significantly (29.9%) due to 100 years return period of rainfall. The biochar application of 10% (B10) can prevent water infiltration to the depth of 0.25 m due to 10 years

return period of rainfall, regarding the constant value of PWP. However, rainfall can infiltrate to the depth of 0.25 m because of 100 years of return periods of rainfall. It also can be reported from Figure (a) that the biochar application of 20% (B20) can hinder water infiltration to the depth of 0.25 m due to all of the return period variation.

Since having higher rainfall intensity compared to the current climate, near future climate resulted from deeper water infiltration depth. Based on the simulation result, rainfall can infiltrate to the depth of 0.25 m during 100-years of return period in a near future climate with all biochar

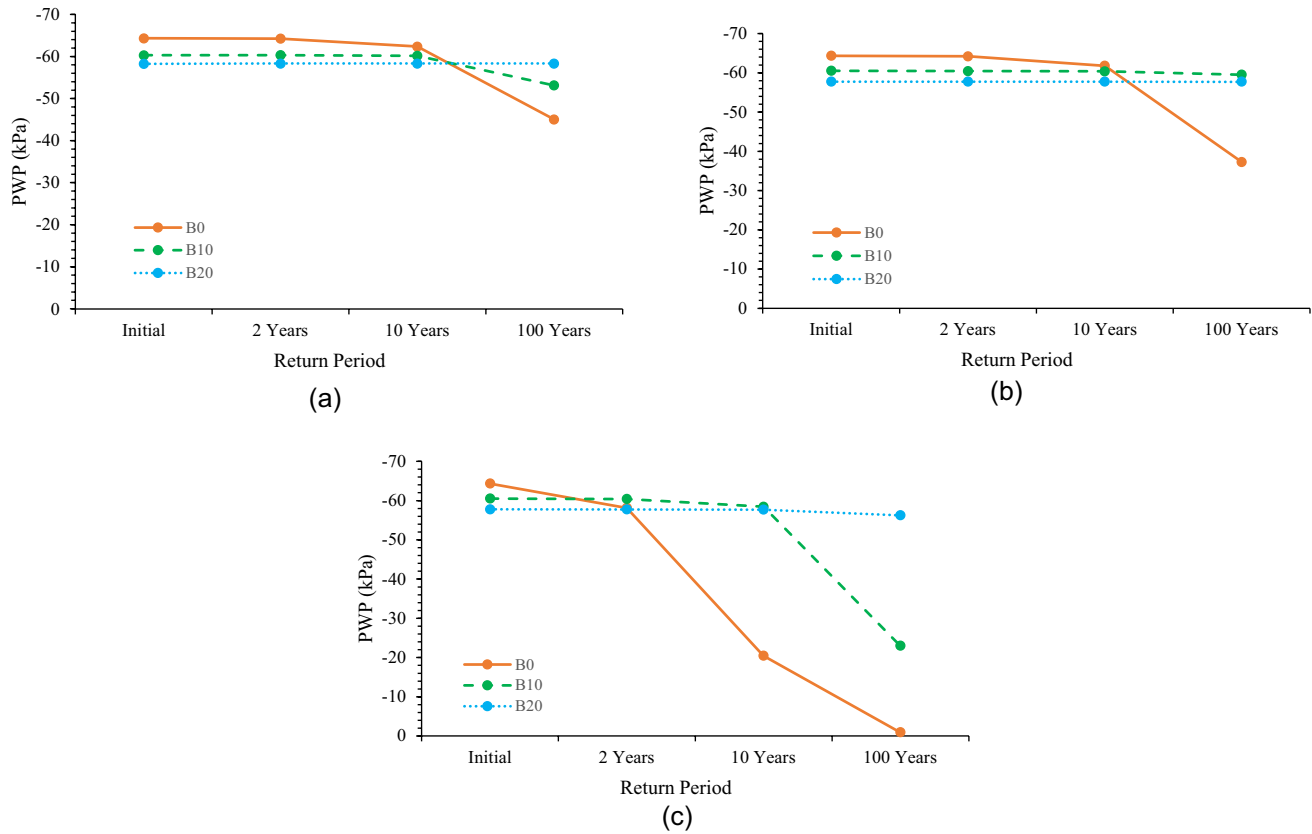


Fig. 7 Development of pore water pressure (PWP) during rainfall with return period and BAS variation **(a)** current climate **(b)** near future climate **(c)** far future climate

composition. To investigate the effect of biochar application under near future climate, the correlation between PWP and return period variation at the depth of 0.45 m was generated, as can be seen in Fig. 7b. Considering Fig. 7b, without biochar application, rainfall infiltrated to the depth of 0.45 m due to a 10-years return period of rainfall, promoting PWP slightly increase by around 3.9%. Moreover, PWP increased by approximately 42% under a 100-years return period of rainfall. Further to this, regarding Fig. 7b, the biochar application of 10 and 20% can maintain water infiltration to the depth of 0.45 m due to a 100-years return period of rainfall. It can be indicated from the stable value of PWP due to all of the return period variations. It substantiated that the biochar application of 10% and 20% can prevent water infiltration up to the upper half of the model during near future extreme climate conditions.

Moreover, the responses of PWP at the depth of 0.45 m with the variation of return period under far future extreme climate conditions can be plotted in Fig. 7c. It can be clearly seen from Fig. 7c that far future extreme climate caused the increase in PWP significantly for soil without biochar composition. Without biochar application, PWP rose by about 9.6% and 68.2% when the model was subjected to 2-years and 10-years

return periods of rainfall. Yet, the PWP value jumped to near 0 kPa as the application of 100-years return period of rainfall. Subtle different PWP responses apparently occurred due to the application of biochar as can be seen in Fig. 7c. The biochar application of 10% can maintain PWP to the depth of 0.45 m under 10-years return period of rainfall. However, PWP also inclined remarkably by approximately 61.9% under 100-years return period of rainfall. Following this, the biochar application of 20% can prevent water infiltration up to the depth of 0.45 under all of the return period variations. With respect to the observed result, it can be concluded that the biochar application of 10% is sufficient enough to prevent water infiltration to the depth of 0.45 due to a 10-years return period of rainfall under near future extreme climate conditions. Further to this, the biochar application of 20% can maintain water infiltration to the depth of 0.45 due to a 100-years return period of rainfall under far future extreme climate conditions.

The effect of biochar variation on water holding capacity

The correlation between biochar composition and VWC for each group of suctions can be depicted in Fig. 8.

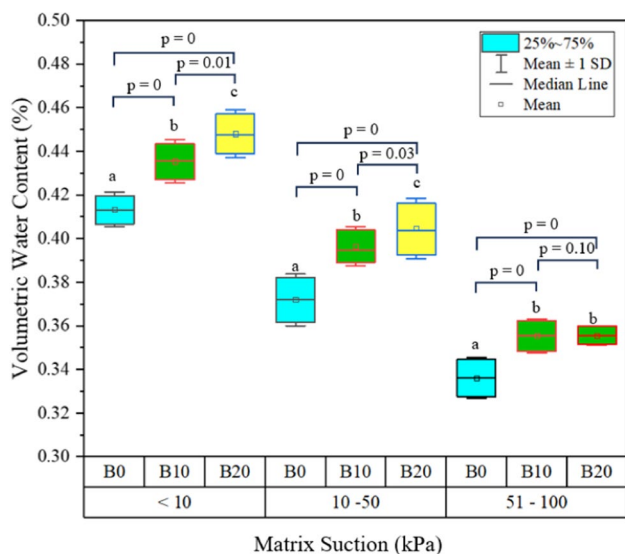


Fig. 8 The effect of BAS variation on soil water holding capacity based on ANOVA test

Figure 8 exhibits that the application of biochar variation resulted in three different groups of water holding capacity at very low (< 10 kPa) and low (10–50 kPa) range suction. Regarding the probability (P) value (< 0.05), each composition of biochar tends to have a different range of VWC, compared to another biochar variations. It represented that the addition of 10 and 20% biochar can significantly affect water retention capacity at very low and low suction ranges. Moreover, it can be reported that the increase in water holding capacity at the middle range of suction (51–100 kPa) due to the addition of 10 and 20% BAS was similar, indicated by the higher P value (> 0.05). It indicated that the addition of 10 and 20% biochar can increase water retention capacity at low matric suction range which can prevent flooding during extreme wet conditions. By adding biochar 10 and 20% can increase water holding capacity by approximately 5.7 and 9.6% respectively. This result is consistent with Qian et al. (2020) which expressed that biochar has the potential to increase soil water holding capacity. Further to this, regarding (Wong et al. (2022), the application of peanut shell biochar increased the soil water holding capacity of clay by > 59% at high matric suction range (48–125 MPa) during severe drought period. This is because biochar has a large surface area and pores, which allow it to be saturated prior to gravitational moisture percolating downward. In addition, the finer biochar particles have the potential to obstruct the sizable soil pores, leading to a subsequent reduction in the rate of water infiltration. Biochar is known for its numerous benefits to soil health, but it's important to recognize that its impact on soil salinity can vary based on its source material and production process (Lee et al. 2022; Liu et al. 2023). Therefore, a

thorough evaluation of biochar's characteristics is essential before large-scale application.

Conclusion

This study evaluated the water infiltration and hydrological behavior of biochar-amended soil (BAS) in extreme climates, using numerical simulation. In this simulation, three variations of Biochar composition (i.e., 0, 10, and 20%) were calculated in response to three extreme climate scenarios (i.e., current, near future, and far future). In this investigation, changes in water infiltration and PWP were observed and studied. The result concluded that biochar amended soil can maintain the fluctuation of PWP due to the wetting and drying process. This is due to the fact that finer particles of biochar may clog large soil pore, reducing the water infiltration rate. Moreover, finer particles of biochar decreased the soil porosity, reducing evaporation area. In detail, the biochar application of 10% and 20% can prevent water infiltration up to depth of 0.25 and 0.45 m respectively under the current extreme scenario. Also, the addition of biochar 10 and 20% is effective in preventing water infiltration to the depth of 0.45 m under near and far future extreme climate scenarios respectively. The study indicates that incorporating 10% biochar into landfill covers, with a thickness of 0.45 m, is an effective strategy for adapting to near-future climate conditions. This approach enhances the resilience of landfill covers under far-future climate scenarios when the biochar composition is increased to 20%. This 20% biochar mix is also capable of managing water infiltration effectively up to a depth of 0.45 m during heavy rainfall events that are predicted to happen once every 100 years in these future climates. This highlights biochar's potential as a climate change adaptation and soil water management technique, especially given its ability to increase soil water holding capacity at lower matric suction ranges (less than 100 kPa). The addition of 20% biochar could thus play a key strategy in flood prevention during periods of excessive rainfall, aligning with sustainable practices for managing water resources in changing climate conditions.

Acknowledgements The corresponding author (V. Kamchoom) acknowledges the grant (RE-KRIS-FF67/007) from King Mongkut's Institute of Technology Ladkrabang (KMITL) and National Science, Research and Innovation Fund (NSRF)

Funding This research was funded by King Mongkut's Institute of Technology Ladkrabang (KMITL) and National Science, Research and Innovation Fund (NSRF) grant number RE-KRIS-FF67/007. The funders had no role in the design of the study; in the collection, analyzes, or interpretation of data; in the writing of the manuscript, or in the decision to publish the results.

Declarations

Conflict of interest The authors declare no conflict of interest.

References

- Abrol V, Ben-Hur M, Verheijen FGA, Keizer JJ, Martins MAS, Tenaw H, Tchekhansky L, Graber ER (2016) Biochar effects on soil water infiltration and erosion under seal formation conditions: rainfall simulation experiment. *J Soils Sedim* 16(12):2709–2719
- Albright WH, Benson CH, Gee GW, Abichou T, Tyler SW, Rock SA (2006) Field performance of three compacted clay landfill covers. *Vadose Zone J* 5(4):1157–1171
- Allen RG, Pereira LS, Raes D, Smith M (1998) *Crop Evapotranspiration-Guidelines for Computing Crop Water Requirements-FAO Irrigation and Drainage Paper 56*. FAO, Rome, 300, D05109
- Anderson MG, Kneale PE (1980) Pore water pressure and stability conditions on a Motorway Embankment. *Earth Surf Process* 5(1):37–46
- Apriyono A, Yuliana and Kamchoom V (2023) Serviceability of cut slope and embankment under seasonal climate variations. *Acta Geophysica* 71:983–995
- ASTM International (2003) Standard method for infiltration rate of soils in field using double-ring infiltrometer. In: *Annual Book of ASTM Standards*, Vol 04.08 Aug, West Conshohocken, pp 4–11
- Borana L, Yin JH, Singh DN, Shukla SK (2017) Influence of matrix suction and counterface roughness on shearing behavior of completely decomposed granitic soil and steel interface. *Indian Geotech J* 47(2):150–160
- Borana L, Yin JH, Singh DN, Shukla SK, Pei HF (2016) Influences of initial water content and roughness on skin friction of piles using FBG technique. *Int J Geomech* 17(4):1–14
- Briggs KM, Dijkstra TA and Glendinning S (2019) Evaluating the deterioration of geotechnical infrastructure assets using performance curves. In: *International Conference on Smart Infrastructure and Construction 2019, ICSIC 2019: driving data-informed decision-making*, vol. 2019, pp 429–435
- Briggs KM, Smethurst JA, Powrie W, O'Brien AS (2013) Wet winter pore pressures in railway Embankments. *Proc Inst Civ Eng Geotech Eng* 166(5):451–465
- Chen Z, Chen C, Kamchoom V, Chen R (2020) Gas permeability and water retention of a repacked silty sand amended with different particle sizes of peanut shell biochar. *Soil Sci Soc Am J* 84(5):1630–1641
- Chen Z, Kamchoom V, Apriyono A, Chen R, Chen C (2022a) Laboratory study of water infiltration and evaporation in biochar-amended landfill covers under extreme climate. *Waste Manag* 153:323–334
- Chen Z, Kamchoom V, Chen R (2022b) Landfill gas emission through compacted clay considering effects of crack pathway and intensity. *Waste Manag* 143:215–222
- Chen Z, Kamchoom V, Chen R, Prasittisopin L (2023a) Investigating the impacts of biochar amendment and soil compaction on unsaturated hydraulic properties of silty sand. *Agronomy* 13:1845
- Chen Z, Kamchoom V, Leung A and Xue J (2023) Influence of biochar on the water permeability of compacted clay subjected to freezing–thawing cycles. *Acta Geophys* 1–11
- Cheng CH, Lehmann J, Engelhard MH (2008) Natural oxidation of black carbon in soils: changes in molecular form and surface charge along a climosequence. *Geochim Cosmochim Acta* 72(6):1598–1610
- Cheng Q, Tang CS, Xu D, Zeng H, Shi B (2021) Water infiltration in a cracked soil considering effect of drying-wetting cycles. *J Hydrol* 593:125640
- Cui G, Zhu J (2017) Infiltration model in sloping layered soils and guidelines for model parameter estimation. *Hydrol Sci J* 62(13):2222–2237
- Cui Y-J, Tang C-S, Tang AM, Ta AN (2014) Investigation of soil desiccation cracking using environmental chamber. *Rivista Italiana Di Geotecnica* 24(1):9–20
- Dong H, Leung AK, Chen R, Lourenco S and Kamchoom V (2023) Changes in pore-size distribution and hydraulic conductivity of compacted soils by grass-derived hydrochar. *J Geotech Geoenviron Eng* 149(9):4023079
- Feng W, Wang T, Yang F, Cen R, Liao H, Qu Z (2023) Effects of biochar on soil evaporation and moisture content and the associated mechanisms. *Environ Sci Eur*. <https://doi.org/10.1186/s12302-023-00776-7>
- Fredlund DG, Rahardjo H (1993) *Unsaturated Soil Mechanics*. Wiley, New York
- Garg A, Huang H, Cai W, Reddy NG, Chen P, Han Y, Kamchoom V, Gaurav S, Zhu HH (2021) Influence of soil density on gas permeability and water retention in soils amended with in-house produced biochar. *J Rock Mech Geotech Eng* 13(3):593–602
- Van Genuchten MT (1980) A closed-form equation for predicting the hydraulic conductivity of unsaturated soils. *Soil Sci Soc Am J* 44(5):892–898
- George C, Wagner M, Kücke M, Rillig MC (2012) Divergent consequences of hydrochar in the plant-soil system: Arbuscular mycorrhiza, nodulation, plant growth and soil aggregation effects. *Appl Soil Ecol* 59:68–72
- Glendinning S, Hughes P, Helm P, Chambers J, Mendes J, Gunn D, Wilkinson P, Uhlemann S (2014) Construction, management and maintenance of embankments used for road and rail infrastructure: implications of weather induced pore water pressures. *Acta Geotech* 9(5):799–816
- Green WH, Ampt GA (1911) Studies on soil physics. *J Agric Sci* 4(1):1
- Hussain R, Ravi K (2022) Investigating biochar-amended soil as a potential lightweight material for embankments. *Ecol Eng* 180:106645
- Ibrahim A, Usman ARA, Al-Wabel MI, Nadeem M, Ok YS, Al-Omran A (2017) Effects of conocarpus biochar on hydraulic properties of calcareous sandy soil: influence of particle size and application depth. *Archiv Agron Soil Sci* 63(2):185–197
- Ibrahim HM, Al-Wabel MI, Usman ARA, Al-Omran A (2013) Effect of conocarpus biochar application on the hydraulic properties of a sandy loam soil. *Soil Sci* 178(4):165–173
- Jin J, Kang M, Sun K, Pan Z, Wu F, Xing B (2016) Properties of biochar-amended soils and their sorption of imidacloprid, Isoproturon, and Atrazine. *Sci Total Environ* 550:504–513
- Joseph S, Cowie AL, Van Zwieten L, Bolan N, Budai A, Buss W, Cayuela ML, Graber ER, Ippolito JA, Kuzyakov Y, Luo Y, Ok YS, Palansooriya KN, Shepherd J, Stephens S, Weng Z, Lehmann J (2021) How biochar works, and when it doesn't: a review of mechanisms controlling soil and plant responses to biochar. *GCB Bioenergy* 13(11):1731–1764
- Kamchoom V, Boldrin D, Leung AK, Sookkrajang C, Likitlersuang S (2022) Biomechanical properties of the growing and decaying roots of *Cynodon dactylon*. *Plant Soil* 471:193–210
- Kamchoom V, Leung AK (2018) Hydro-mechanical reinforcements of live poles to slope stability. *Soils Found* 58(6):1423–1434
- Lagmago KL (2021), Investigation of sand-biochar mixtures as a potential roadway fill material, Louisiana State University, https://digit.alcommons.lsu.edu/gradschool_theses/5443/
- Lee X, Yang F, Xing Y, Huang Y, Xu L, Liu Z, Holtzman R, Kan I, Li Y, Zhang L, Zhou H (2022) Use of biochar to manage soil salts and water: Effects and mechanisms. *Catena* 211:106018
- Lees AS, MacDonald GJ, Sheerman-Chase A, Schmidt F (2013) Seasonal Slope movements in an old clay fill Embankment dam. *Can Geotech J* 50(5):503–520

- Lehmann J and Joseph S (2009) Biochar for environmental management: an introduction. In: *Biochar for Environmental Management: Science and Technology*, Earthscan 5 August, London, <http://downloads.esri.com/archydro/archydro/Doc/OverviewofArcHydroterrainpreprocessingworkflows.pdf%0A10.1016/j.jhydrol.2017.11.003%0Ahttp://sites.tufts.edu/gis/files/2013/11/Watershed-and-Drainage-Delineation-by-Pour-Point.pdf%0Awww>
- Leroueil S (2001) Natural slopes and cuts: movement and failure mechanisms. *Geotechnique* 51(3):197–243
- Liu Q, Meki K, Zheng H, Yuan Y, Shao M, Luo X, Li X, Jiang Z, Li F, Xing B (2023) Biochar application in remediating salt-affected soil to achieve carbon neutrality and abate climate change. *Biochar* 5:45
- Ng CWW, Leung AK, Yu R, Kamchoom V (2017) Hydrological effects of live poles on transient seepage in an unsaturated soil slope: centrifuge and numerical study. *J Geotech Geoenviron Eng* 143(3):1–9
- Novak J, Sigua G, Watts D, Cantrell K, Shumaker P, Szogi A, Johnson MG, Spokas K (2016) Biochars impact on water infiltration and water quality through a compacted subsoil layer. *Chemosphere* 142:160–167
- Passioura JB (2002) Soil conditions and plant growth. *Plant, Cell Environ* 25(2):311–318
- Penman HL (1948) Natural evaporation from open water, bare soil and grass. *Proc R Soc Lond Ser A, Math Phys Sci* 193(1032):120–145
- Pham TA, Sutman M, Medero GM (2023) Validation, reliability, and performance of shear strength models for unsaturated soils. *Geotech Geol Eng* 41:7
- Qian Z, Tang L, Zhuang S, Zou Y, Fu D, Chen X (2020) Effects of biochar amendments on soil water retention characteristics of red soil at South China. *Biochar* 2(4):479–488
- Qiao C, Ning Z, Wang Y, Sun J, Lin Q, Wang G (2021) Impact of climate change on water availability in water source areas of the South-to-North water diversion project in China. *Front Earth Sci* 9:1–9
- Ramezanzadeh H, Zarehaghi D, Baybordi A, Bouket AC, Oszako T, Alenezi FN, Belbahri L (2023) The Impacts of biochar-assisted factors on the hydrophysical characteristics of amended soils: a review. *Sustainability (switzerland)* 15(11):1–25
- Ranjan G and Rao ASR (2000) *Basic and Applied Soil Mechanics*, New Age International Publishers, New Delhi, <https://books.google.com/books?id=U2AvQrA6I4sC&pgis=1>
- Razzaghi F, Obour PB, Arthur E (2020) Does biochar improve soil water retention? A systematic review and meta-analysis. *Geoderma* 361:114055
- Shang G, Shen G, Liu L, Chen Q, Xu Z (2013) Kinetics and mechanisms of hydrogen sulfide adsorption by biochars. *Bioresour Technol* 133:495–499
- Shrestha A, Babel MS, Weesakul S, Vojinovic Z (2017) Developing intensity-duration-frequency (IDF) curves under climate change uncertainty: the case of Bangkok, Thailand. *Water (switzerland)*. <https://doi.org/10.3390/w9020145>
- Smethurst JA, Clarke D, Powrie W (2006) Seasonal changes in pore water pressure in a grass-covered cut slope in London Clay. *Geotechnique* 56(8):337–351
- Song WK, Cui YJ (2020) modeling of water evaporation from cracked clayey soil. *Eng Geol* 266:105465
- The World Bank Group and The Asian Development Bank (2021) *Climate Risk Country Profile: Thailand*
- Uzoma KC, Inoue M, Andry H, Fujimaki H, Zahoor A, Nishihara E (2011) Effect of cow manure biochar on maize productivity under sandy soil condition. *Soil Use Manag* 27(2):205–212
- Wang ZC, Zhang BW, Ni JX, Yang WH, Li WP (2022) Effect of microplastics on soil water infiltration and evaporation. *Huanjing Kexue/environ Sci* 43(8):4394–4401
- Wong JTF, Chen Z, Chen X, Ng CWW, Wong MH (2017) Soil-water retention behavior of compacted biochar-amended clay: a novel landfill final cover material. *J Soils Sedim* 17(3):590–598
- Wong JTF, Chow KL, Chen XW, Ng CWW, Wong MH (2022) Effects of biochar on soil water retention curves of compacted clay during wetting and drying. *Biochar* 4(1):1–14
- Yamoat N, Hanchoo Wong R, Sriboonlue S, Kangrang A (2022) Temporal change of extreme precipitation intensity–duration–frequency relationships in Thailand. *J Water Clim Change* 13(2):839–853
- Yu L, Tang J, Zhang R, Wu Q, Gong M (2013) Effects of biochar application on soil methane emission at different soil moisture levels. *Biol Fertil Soils* 49(2):119–128
- Zeng H, Tang CS, Cheng Q, Zhu C, Yin LY, Shi B (2020) Drought-induced soil desiccation cracking behavior with consideration of basal friction and layer thickness. *Water Resour Res* 56(7):1–15

Springer Nature or its licensor (e.g. a society or other partner) holds exclusive rights to this article under a publishing agreement with the author(s) or other rightsholder(s); author self-archiving of the accepted manuscript version of this article is solely governed by the terms of such publishing agreement and applicable law.